

Xenon DNP in Inhomogeneous Solid-State Mixtures: Elucidation of the Spin-Diffusion Bottleneck

Mehrdad Pourfathi¹, Nicholas N Kuzma¹, Rajat K Ghosh¹, Stephen Kadlecck¹, and Rahim Rizzi¹
¹Department of Radiology, University of Pennsylvania, Philadelphia, PA, United States

Introduction: The limited availability of ³He gas and its rapidly rising cost have inhibited further adaptation of hyperpolarized-gas MRI for assessment of lung function and structure. To address this limitation, we have recently developed a technique to produce large quantities of an alternative imaging agent, ¹²⁹Xe gas hyperpolarized by dynamic nuclear polarization (DNP). However, the levels of ¹²⁹Xe polarization vary significantly and are still considerably lower than those achieved in pyruvate-like molecules under identical DNP conditions. This discrepancy in experimental findings may be attributed to the inaccessibility of the microscopic DNP parameters (such as local relaxation and polarization rates) in the glassy solid-state mixtures used for Xe DNP [1,2]. The data collected in our recent experiments [3] offer an opportunity to distinguish the populations of ¹²⁹Xe spins belonging to the different compartments in partially-segregated solid-state DNP mixtures, by resolving the different ¹²⁹Xe chemical shifts and dipolar broadening values inside and outside of spontaneously occurring pure-¹²⁹Xe clusters. Our early experiments presented a peculiar time evolution of one of the ¹²⁹Xe NMR peaks, indicating a severe spin diffusion bottleneck at the cluster boundaries. An empirical model was then developed to explain the combined effects of the nuclear spin diffusion and *T*₁ relaxation on the evolution of DNP in these xenon clusters. Unfortunately, that earlier model did not provide any insight into the nature of the postulated polarization bottleneck. In this work, we present a self-contained analysis that properly accounts for the spatial inhomogeneity of ¹²⁹Xe polarization inside the glassy matrix. Theoretical fitting to the experimental spin-up and spin-down curves now explains the origin of the spin-diffusion bottleneck in terms of the basic microscopic DNP parameters, providing a valuable local probe for evaluating the internal mechanism of the DNP process.

Materials and Methods: We assumed spherical pure-xenon clusters with an unknown radius, *R*₁, surrounded by a matrix of ¹²⁹Xe/1-propanol/Finland-acid radical at temperature, *T*. The space-averaged polarization outside the clusters was measured to saturate exponentially during spin-up and spin-down DNP [3]. To account for the inhomogeneity of local polarization across the glassy matrix, we divided the total inter-cluster volume into cells approximated as spheres with an unknown radius, *R*₂, concentric with each cluster (Fig. 1A). The ratio *R*₂/*R*₁ = 1.49 was calculated from the known concentrations and thermal magnetizations [4]. Inside the cluster (*r* < *R*₁), ¹²⁹Xe polarization obeyed the spin-diffusion equation (Eq. 1) where the nuclear spin diffusion coefficient was *D*_{s1} ≈ 7.3 × 10⁻¹⁴ cm²/s [3]. Eq. 2 models the time-evolution of local polarization in the glassy matrix of a spherical shell as an interplay of spin diffusion and DNP. Here *P*^{*}_{DNP} = 6.22% (*P*_{DNP} = -5.47%) are the effective ultimate local polarizations during DNP at *v*⁺ and *v*⁻ microwave frequencies [4], and *D*_{s2} ≈ *D*_{s1} / 77.4 is the independently estimated spin-diffusion coefficient in the glassy matrix [4]. Eqs. 4-6 define the initial and boundary conditions. Continuity of local polarization across the glassy matrix is represented by Eq. (5). Eq. (6) enforces conservation of the magnetization flux across the cluster/matrix boundary, where *n*₁ and *n*₂ are Xe concentrations inside and outside the clusters. Eq. (7) provides the normalization of ¹²⁹Xe polarization of Eq. (2) to the NMR volume-averaged data during DNP.

Results and Discussion: Experimentally measured area under the narrow peak in the spectrum (Fig. 1B) is shown by filled and open circles in Figs. 2A,B. Our model reproduces the time evolution of ¹²⁹Xe polarization by fitting the volume-averaged local polarization estimated from Eq. 1 (solid and dashed lines in Fig. (2A,B)) to the experimental data. From the fit, we infer the following cluster parameters: cluster radius *R* ≈ 1.21 ± 0.04 μm, spin relaxation inside the cluster *T*₁ = 167 ± 7 min and the thermal polarization *P*₀ = 0.051 ± 0.001 %. The experimental NMR spectra show that polarization inside the cluster is on the order of the thermal polarization, whereas in the matrix enhancement by a factor of 30 is observed compared to thermal polarization (Fig 1D). In the previous model [3], this mismatch between the polarization levels was accommodated by postulating a polarization bottleneck constant in the boundary condition of the intra-cluster polarization. This bottleneck was deemed to be a result of the poor spectral overlap between the broad and narrow ¹²⁹Xe NMR peaks corresponding to the matrix and the clusters (Figs. 1B and 1C). In this work, this mismatch is explained by Eq. 6 as the result of the polarization drop in a thin “insulating” layer of the matrix immediately surrounding the cluster. The insulating property of the layer stems from the very low ¹²⁹Xe spin diffusion constant compared to that of pure xenon, which can be independently calculated based on the concentration of xenon atoms in the matrix and the corresponding ¹²⁹Xe-¹²⁹Xe distances inside and immediately outside of the pure-Xe cluster.

Conclusion: Our self-contained local DNP model is now very sensitive to the cluster size, since there is no need to introduce an unknown “bottleneck constant”. Previously, the cluster size and the bottleneck constant values obtained from the fit were statistically strongly coupled, resulting in large uncertainties in each value. The current model also shows a high sensitivity to the intrinsic sample temperature and a fair sensitivity to *T*₁ in the clusters. The fitting of the parameters of the model to the experimental data shows that the cluster radius is about a micron. Furthermore, our findings support our earlier hypothesis on the “polarization discontinuity” at the boundary of the cluster in the DNP of solid ¹²⁹Xe samples. We can find the intrinsic temperature of the xenon sample during DNP to be *T* = 2.74 ± 0.05 K. This is much higher than the ambient temperature of the helium bath. This finding, based entirely on the prediction of the numerical model developed here, has led to several modifications of our DNP system with the goal to reduce overheating (such as eliminating thermal barriers to cooling, lowering microwave power, and pelletizing the sample), and resulted in the increase of maximum ¹²⁹Xe polarization from 5.1% to 21% [3].

Acknowledgment of support by NIH R01 EB010208. **References:** [1] J.-H. Ardenkjaer-Larsen et al., US patent 8,003,077, filed 2003, issued 2011. [2] A. Comment et al., Phys. Rev. Lett. 105, 018104 (2010). [3] N. N. Kuzma et al., J. Chem. Phys. 137, 104508 (2012). [4] M. Pourfathi et al., J. Chem. Phys. 2012 (submitted).

$$\frac{\partial P(r,t)}{\partial t} = D_{s1} \nabla^2 P(r,t) + \frac{P_0 - P(r,t)}{T_1}, 0 < r < R_1 \quad (1)$$

$$\frac{\partial P(r,t)}{\partial t} = D_{s2} \nabla^2 P(r,t) + \frac{P_{DNP} - P(r,t)}{T_{su}}, R_1 < r < R_2 \quad (2)$$

$$|P(0,t)| < 1 \quad (3), \quad P(r,0) = 0 \quad (4), \quad \frac{\partial P(R_2,t)}{\partial r} = 0 \quad (5)$$

$$n_1 D_{s1} \frac{\partial P(R_1 - \delta r)}{\partial r} = n_2 D_{s2} \frac{\partial P(R_1 + \delta r)}{\partial r} \quad (6)$$

$$\langle P_{avr}(t) \rangle = \left(\frac{4}{3} \pi (R_2^3 - R_1^3) \right)^{-1} \int_{R_1}^{R_2} P(r,t) 4\pi r^2 dr \quad (7)$$

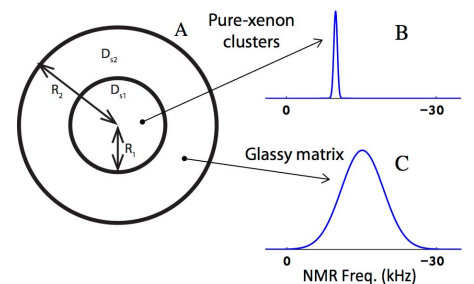


Figure 1. A: Sketch of pure-xenon cluster surrounded by a spherical shell of solid xenon/1-propanol/trityl mixture. B: The narrow peak in the NMR spectrum corresponds to pure xenon clusters. C: The broad peak represents xenon/1-propanol/trityl mixture.

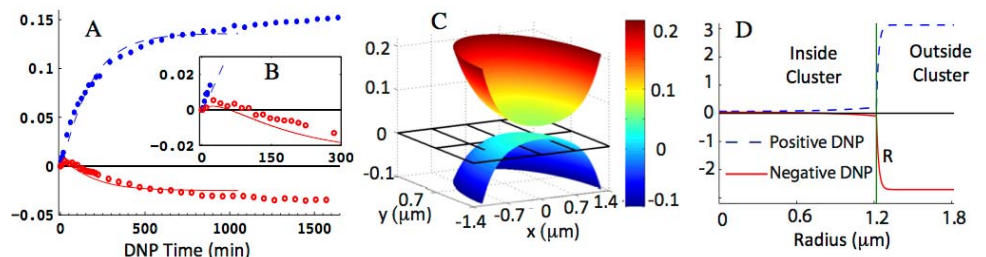


Figure 2. A. Experimentally measured volume-averaged polarization in pure-xenon clusters as a function of time for positive and negative DNP (filled and open circles). Simultaneous fitting of the data using the model. The inset B shows close-up views of the cluster-average polarization within minutes after initiating DNP. Note the peculiar behavior of polarization for 0 < *t* < 120 min under negative DNP and the quality of the fit using the model. C. Modeled polarization profiles across the spherical cluster at time *t* = 1024 min. D. Corresponding radial dependence of ¹²⁹Xe polarization according to the model. Note the non-smooth continuity at the boundary of the cluster at *r* = 1.2 μm, representing the earlier postulated polarization bottleneck at the cluster boundary.